Interaction and Multiscale Mechanics, Vol. 5, No. 2 (2012) 145-155
DOI: http://dx.doi.org/10.12989/imm.2012.5.2.145

The Application of welding numerical simulation on two typical welded structures in railway vehicles

Li Ya-na*[1], Li Cheng-tao[1], Yuan Bin[2] and Xie Su-ming[1]

[1]*Traffic and Transportation School, Dalian Jiao tong University, Dalian, China*
[2]*Transportation Equipments and Ocean Engineering College, Dalian Maritime University, Dalian, China*

(Received August 22, 2011, Revised April 19, 2012, Accepted April 23, 2012)

Abstract. The thin-plate structure and the box-beam structure are two typical welded structures in railway vehicles. Because of their structure complexity, bigger size and multi-seams, welding residual distortion which occur in welding process bring unfavorable effect on the quality of welding products manufacturing and service. As a result, welding distortion forecasting and control become an important and urgent research topic in railway vehicles. In this paper, three different numerical methods are presented corresponding to three typical types of welded structures of railway vehicles and welding deformation are simulated. Consistence of numerical results and experimental data proves the correctness of models and feasibility of simulation methods.

Keywords: thin-plate structure; box-beam structure; railway vehicle; welding distortion; numerical simulation methods.

1. Introduction

Welding technology in cars, ships, nuclear reactors, railway vehicles and aerospace industries has been employed at an increasing rate for its advantages in design flexibility, cost saving, reduced overall weight and enhanced structural performance. However, welding induces stresses which result into various types of distortion, as discussed in detailed by Masubuchi (1980). To assess the effects of welding on structure efficiently, and in turn to implement various distortion mitigation techniques, validated methods to predict welding induced deformation are necessary.

With the development of welding simulation and computer technology, the numerical simulation method will more and more play an important role. It starts from analytical method, gradually transits to finite difference method, finite element method, numerical integral method *et al*. In recent years, the finite element method has been the dominant status because of the development of finite element software and its good effect. The numerical simulation becomes the main research method for the welding deformation. These methods are summed up: inherent stain method (Ueda *et al.* 1992, Takeda 2002), thermo-elastic-plastic finite element method (Masubuchi *et al*. 1996, Michaleris 2006), finite element method considering phase transition and various coupling effect

* Corresponding author, Associate Professor, E-mail: lyn@djtu.edu.cn

(Oddy *et al*. 1900, Leblond *et al.* 1986), viscous elastic-plastic finite element method (Nied 1993), “local-global” finite element method (Tsirkas *et al.* 2003, Jeong 2011) *et al.*

Although the numerical simulation studies on welding distortion have been conducted for many years at home and abroad from the years 1960s, less research work for welding structures in railway vehicles is done, especially in considering large-scale complex welded structures. In this paper, three numerical methods for three typical applications of railway vehicles are presented. Consistence of numerical simulation results and experiments data proves the correctness of models and feasibility of simulation methods.

2. Numerical simulation methods

2.1 Equivalent thermal load method

The thin-plate buckling deformation is extremely easy to occur in the welding process. It is a technical problem in welding procedure because of the complication and diversity of the deformation. Many experts and scholars, at home and abroad, use methodologies of numerical simulation to perform much study on buckling deformation and make a number of important achievements. The main research methods (Junxia *et al.* 2005, Michaleris *et al.* 1997, Xinqi *et al.* 2002) are summarized as follows: (1) thermal-elastic-plastic finite element method of small deformation for 2D or 3D, (2) thermal-elastic-plastic finite element method of large deformation for 3D, (3) plastic strain finite element method for decoupling 2D-3D, (4) equivalent thermal loads method based on the inherent strain. The fourth method is fit for the buckling calculation of the thin-plate structure.

According to the characteristics of thin-plate welded structure, an equivalent thermal load method based on inherent strain is put forward.

The loading P_{app} caused by welding temperature field in the welding process can be expressed as

$$P_{app} = -E\alpha A_{weld}\Delta T_w \tag{1}$$

$$\Delta T_w = \varepsilon/\alpha \tag{2}$$

Where E is elastic modulus, A_{weld} is weld area, ΔT_w is equivalent thermal loading, α is linear expansion coefficient and ε is longitudinal inherent strain. The relation between longitudinal inherent strain ε and the heat input Q can be expressed as

$$\varepsilon = \frac{KQ}{F} \tag{3}$$

Where F is the distributional area of the total strain.

The heat input Q can be expressed as

$$Q = \frac{\eta UI}{V} \tag{4}$$

Where η is coefficient, U is voltage, I is current, V is welding speed.

$$K = \frac{(0.255 \sim 0.355)\alpha}{c\rho} \tag{5}$$

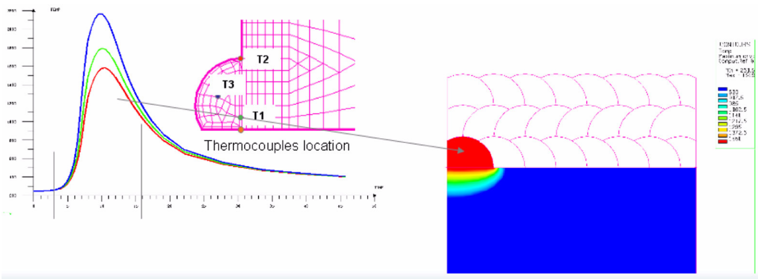

Fig. 1 Computed and measured thermal cycle curves

Where c is specific heat, ρ is density and K is coefficient, usually can be used as $8.6 \times 10^{-7} cm^3/J$ in the welded structure made by low carbon steel or low metal alloy steel.

2.2 Multi-pass prescribed thermal cycle load method

In the thick plate welding, multi-layer and multi-pass welding processes are generally used in order to ensure welding quality, reduce the welding residual deformation and residual stress. But heat and mechanical calculation are very large when using the transient heat source to solve distortion, so heat source model must be simplified.

According to the characteristics of multi-pass (Qingguo *et al.* 2005) box welded structure, a heat source treatment method of multi-pass welding based on thermal-elastic-plastic theory is put forward. First, every thermal cycle curve of seams is obtained by using heat source adjust model of local joint as show in Fig. 1. Second, thermal cycle load extracted from the 3D simulation of local joint model is applied on each bead of the global model for multi-pass simulation. The thermal cycle load is characterized by using a standard transient welding simulation. In order to simulate heat source moving along welding line, thermal load process can be divided into several small periods in accordance with the time on each bead. The advantage of this method is to strongly reduce the computation time. This is a great advantage due generally to the size of the model and due to the number of passes.

2.3 Local-global finite element method

Considering the high gradients of temperature, phases, stresses and plastic strains located in small areas which are involved in welding simulation, the refinement of meshes near the welding line increases drastically models size. With this technique, a model of a railway vehicle would require millions of nodes and even with extremely powerful computers, it does not seem realistic to perform a complete computation in reasonable time. In this paper, we present a new methodology to perform complex 3D welding simulations in order to calculate residual distortions of shell structures.

According to the characteristics of large size box-beam welded structure, a “local-global” project FEM method and mcroelements technology are put forward.

It is first assumed that metallurgical structure and plastic strains locally induced by the welding heat source only depend on local thermal and mechanical conditions. It is therefore possible to compute the residual plastic strains using a local 3D model. 2D model can even be used in some

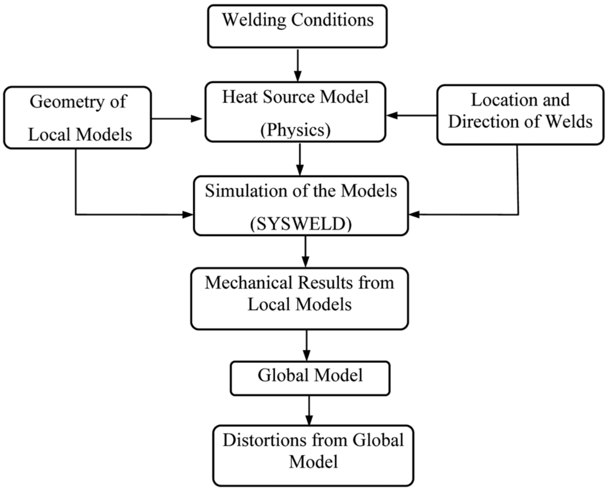

Fig. 2 Flow chart of local – global approach

cases. Then, considering the structure after complete cooling and unclamping, the stress field can be locally expressed as

$$\sigma = E \cdot (\varepsilon - \varepsilon^{p}) \tag{6}$$

where E is the elasticity matrix, ε is the total strain and ε^{p} is the plastic strain as computed by the local analysis respectively. Therefore, the residual stresses and strains on the global model can be computed using an elastic simulation applying ε^{p} as initial strains. These plastic strains are applied along the welding paths on the global model using macroelements. Let's call this methodology the local-global approach (B. Souloumiac *et al.* 2002, Tsirkas *et al.* 2003).

The steps taken for the evaluation of the final distortions of the structure are shown schematically in Fig. 2.

3. Case study

3.1 Application of welding deformation simulation on the truck side-wall

The thickness of the truck side-wall is about 3-6 mm, far less than its length (10000 mm) and width (2700 mm). In the welding process, due to compressive stress caused by shrinkage force in the weld seams, side-wall become instable and produce wave deformation. According to the actual welding process and technical parameters, equivalent thermal load can be calculated using Eq. (1) and Eq. (2) to simulate buckling and large deformation of truck side-wall with ANSYS software considering welding sequences and boundary conditions.

Due to welding load is greater than critical buckling load, on the sidewalls the bucking deformation are produced. First buckling factor is 0.523 and bucking mode is shown in Fig. 3. In order to study the magnitude of deformation, the large deformation is further calculated. The magnitude of the deformation is shown in Fig. 4.

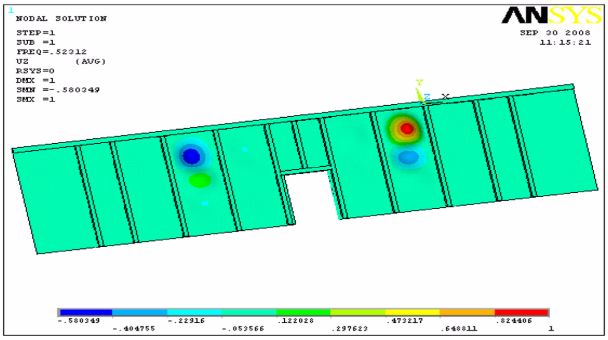

Fig. 3 First bucking mode

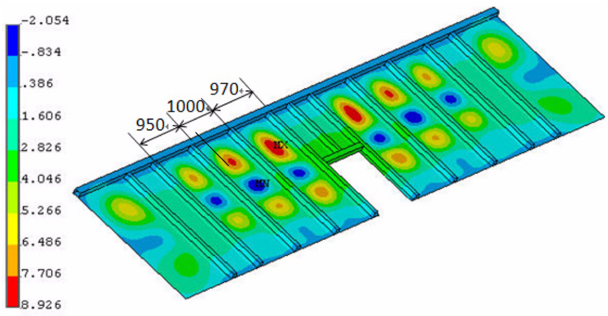

Fig. 4 Welding deformation

Table 1 Experimental and numerical values

Spacing width / Results	950 *w*/mm	970 *w*/mm	1000 *w*/mm
Simulation results	7.14	9.02	8.46
Experimental results	6~10	7~10	8~10

Based on the flatness measurement of fifty sidewalls, the results in three span range are counted respectively. The results of the measurement and the simulation are given in Table 1.

The consistence of simulation results with the measured results proves the correctness of the simulation model and the feasibility of the methodology.

3.2 Application of welding deformation simulation on the side beam

Welding deformations of side beam on bogie frame are studied using multi-pass prescribed thermal cycle load with SYSWELD software.

Heat source model

The heat input to the weld is generally calculated from the energy supplied. The heat input distribution will determine the size and shape of the weld pool. To simulate the heat distribution and

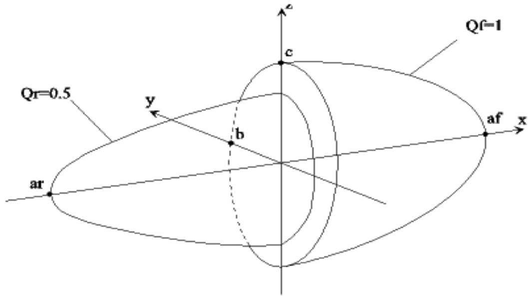

Fig. 5 Double ellipsoidal model

flow in the welding direction, the model of the heat source assumes a double ellipsoid heat flux distribution on the weld pool (as shown in Fig. 5). This model has the capability to be changed by the simple adjustment of various geometrical parameters to simulate different weld pools that correspond to different welding parameters.

Double ellipsoid heat source can be divided into two section, front and back heat flux distribution are expressed as

$$Q(x,y,z) = Q_f \exp\left(-\left(\frac{x^2}{a_f^2}+\frac{y^2}{b^2}+\frac{z^2}{c^2}\right)\right)$$

$$Q(x,y,z) = Q_r \exp\left(-\left(\frac{x^2}{a_r^2}+\frac{y^2}{b^2}+\frac{z^2}{c^2}\right)\right) \tag{7}$$

where Q_f is input energy of front double ellipsoidal, Q_r is input energy of rear double ellipsoidal, a_f is the length of front double ellipsoidal, a_r is represent the length of rear double ellipsoidal, b is weld width, c is weld penetration depth.

Extract thermal cycle curve

Through the heat source calibration of local joint model (see Fig. 6), first pass thermal cycle curve is obtain use double ellipsoidal heat source model. The thermal cycle is the average value of all thermal cycle by all nodes in the bead as show in Fig. 7. Other pass thermal cycle curves can be got by the same way.

Simulation results

The results of the side beam simulation are shown in Fig. 8. The results of the simulation are compared with experimental measurement of distortions which have been performed. Vertical displacement of experimental and numerical values on both sides of the structure are shown in Fig. 9. The consistence of simulation results with the measured results proves the correctness of the simulation model and the feasibility of the methodology.

Fig. 6 Heat source calibration

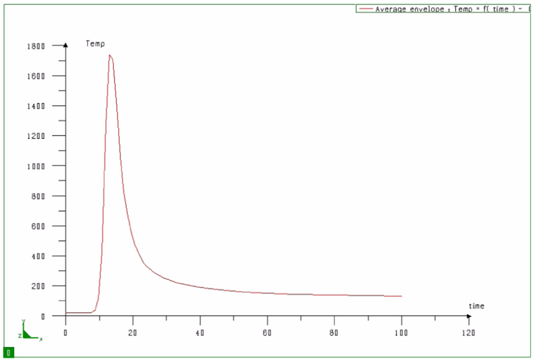

Fig. 7 Thermal cycle curve

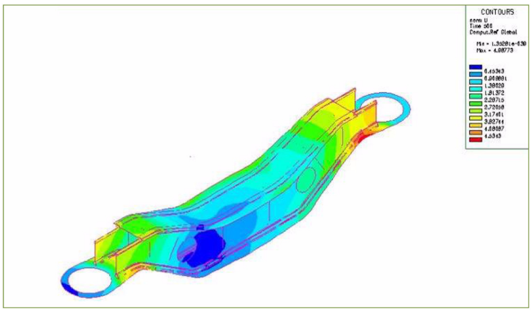

Fig. 8 Vertical displacement

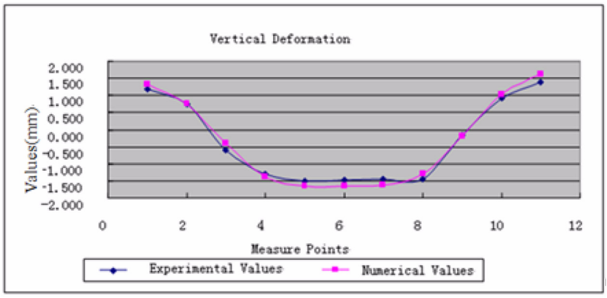

Fig. 9 Experimental and simulation value

Table 2 Heat source model parameters

Parameters	1	2	3	4
Q (J)	4928	14535	7840	14535
a_f (mm)	3	3	3	3
a_r (mm)	4	4	4	4
b (mm)	3	5	3	5
c (mm)	4	3	4	3
a_y (°)	50	30	50	45
v (mm/s)	5	7.5	5	7.5
η	0.8	0.85	0.8	0.85
Q_f	35	85	56	87
Q_r.	23	57	37	58

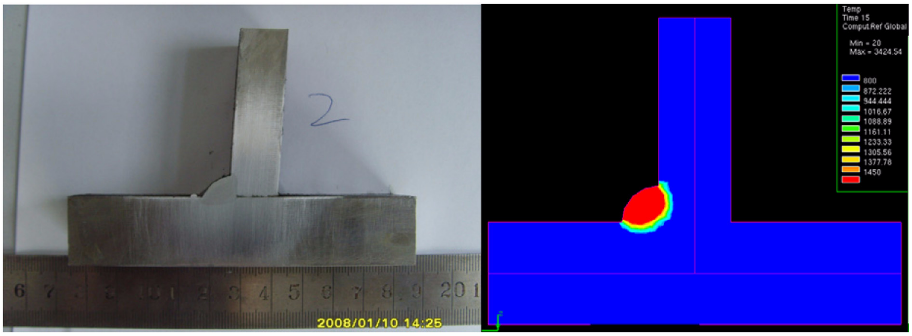

Fig. 10 Heat source calibration model

3.3 Application of welding deformation simulation on middle beam

Welding deformations of middle beam on container underframe are studied using local-global approach with Pam-assembly software.

Heat source model

According structure size and welding processes, parameters of four heat sources calibration with double ellipsoid model are obtained with SYSWELD software (in Table 2).

One of heat source model calibration is shown in Fig. 10.

Local model

It is assumed that plastic strains induced by the welding process are located close to the welding path and depend only on local thermal and mechanical conditions. It is therefore possible to compute these residual plastic strains using a local three-dimensional model. In the simulation of middle beam, four local models with different welding parameters are prepared to be used. One of the strain distribution obtained is shown in Fig. 11.

Global model

The whole structure is 18400 mm long, 800 mm high and 500 mm wide. The finite element model

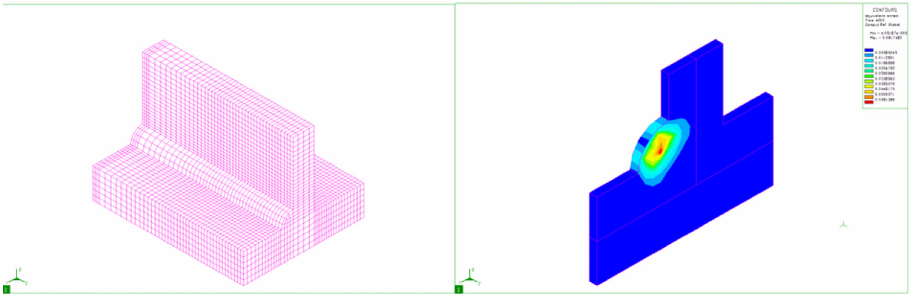

Fig. 11 Local joint strain model

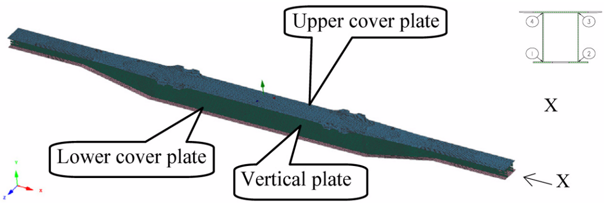

Fig. 12 Finite element model

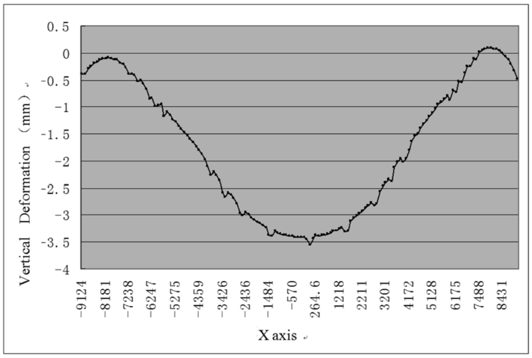

Fig. 13 Longitudinal bending deformation

is 37766 elements and 38642 nodes include 6 parts, 40 welding lines and 4 fix nodes, as shown Fig. 12.

The residual stresses and distortions of the whole structure (global model) can be computed using an elastic simulation applying ε^{p} as initial strains. This task is performed in two steps as follows:

(1) each local model is transformed into a specific finite element, termed the welding macroelement (WME), using a "super element" like technique.

(2) each WME is then linked to the global structure consisting of shells.

Simulation results

Through the calculation, longitudinal bending deformation of middle beam is evident, but transverse shrinkage and rotational deformation are not great. The biggest value of longitudinal bending deformation is −3.552 mm, the whole deformation curve along the X axis is shown in Fig. 13. In the experimental measurement of middle beam, the values of longitudinal bending deformation are between 3 mm and 5 mm. The consistence of simulation results with the measured results proves the correctness of the simulation model and the feasibility of the methodology.

4. Conclusions

Thin-plate welding deformation is a kind of problem, multi-pass welding deformation simulation is another problem, large-scale welding deformation is more difficult numerical simulation problem. In this paper, according three typical welding structures, three numerical simulation methods: equivalent thermal load, multi-pass prescribed thermal cycle load and "local-global" FEM are put forward for realizing welding simulation on railway vehicles. These numerical simulation methods are helpful for mastering the regularity of welding distortion, and also provide technical support for the design, making and optimization of railway vehicle welding process.

Acknowledgments

This work has been partially sponsored by International cooperation project of "high-speed train development 380 km/h" (Grant No. 2010DFB80050-1), National 863 plan project of "professional component and system development of complex equipment operation and maintenance services" (Grant No. 2012AA040912), Ministry of railways project of "van fatigue test technology research" (Grant No. 2011J014-B).

References

Jeong, K.M., Beom, H.G., Kim, K.W. and Cho, J.R. (2011), "Fatigue life prediction for radial truck tires using a global-local finite element method", *Interact. Multiscale Mech.*, **4**(1), 35-47.

Junxia Yan, Lixing Huo, Yufeng Zhang, *et al.* (2005), "Prediction method of buckling distortion of welding thin-plate", *Transactions China Weld. Inst.*, (6), 50-53.

Leblond, J.B., Mottet, G. and Devaux, J.C. (1986), "A theoretical and numerical approach to the plastic behavior of steels during phase transformations - I. Derivation of general relation [J]", *J. Mech. Phys. Solids*, **34**(4), 395-409.

Masubuchi, K. (1980), "Analysis of welded structures", Oxford, Pergamon Press.

Masubuchi, K. (1996), "Prediction and control of residual stresses and distortion in welded structures [J]", *Proc. Theoretical Prediction in Joining and Welding*, 71-88.

Michaleris, P. and Debiccari, A. (1997), "Prediction of welding distortion", *Weld. Res. Suppl.*, (4), 172-181.

Michaleris, P., Zhang, L., Bhide, S.R. and Marugabandhu, P. (2006), "Evaluation of 2D, 3D and applied plastic strain methods for predicting buckling welding distortion and residual stress [J]", *Sci. Technol. Weld. Joi.*, **11**(6), 707-716.

Nied, H.A. (1993), "Finite element simulation of the upset welding process [J]", *J. Eng. Gas Turb. Power*, Transactions of the ASME, **115**(1), 184-192.

Oddy, A.S., McDill, J.M.J. and Goldak, J.A. (1990), "Consistent strain fields in 3D finite element analysis of welds [J]", *J. Press. Vess-T ASME*, **112**(3), 309-311.

Qingguo, M., Hongyuan, F. and Janguo, Y. (2005), "Numerical simulation of multipass welding's temperature field and study of temperature distribution rules", *Chinese J. Mech. Eng.*, **41**(1), 124-128.

Rojek, J. and Onate, E. (2007), "Multiscale analysis using a coupled discrete/finite element model", *Interact. Multiscale Mech.*, **1**(1), 1-31.

SYSWELD® (2010), User's manual, ESI Group.

Takeda, Y. (2002), "Prediction of butt welding deformation of curved shell plates by inherent strain method [J]", *J. Ship Prod.*, **18**(2), 99-104.

Tsirkas, S.A., Papanikos, P., Pericleous, K., Strusevich, N., Boitout, F. and Bergheau, J.M. (2003), "Evaluation of distortions in laser welded shipbuilding parts using local-global finite element approach", *Sci. Technol. Weld. Joi.*, **8**(2), 79-88.

Ueda, Y., Murakawa, H., Gu, S. and Okumoto, Y. (1992), "Simulation of welding deformation for accurate ship assembling (1st Repost) In-plane deformation of butt welded plate", *J. Soc. Nav. Archit. Japan*, **171**, 395-404.

Xinqi, Y. and Lixing, H. (2002), "Prediction analysis of buckling distortion of thin-plate structure", *China Weld.*, (11), 138-142.